Thermochimica Acta 473 (2008) 45–49

Contents lists available at ScienceDirect

Thermochimica Acta

journal homepage: www.elsevier.com/locate/tca

A study on isothermal kinetics of thermal decomposition of cobalt oxalate to cobalt

S. Majumdar*, I.G. Sharma, A.C. Bidaye, A.K. Suri

Materials Group, Bhabha Atomic Research Centre, Trombay, Mumbai 400085, India

ARTICLE INFO

Article history:
Received 13 December 2007
Received in revised form 31 March 2008
Accepted 7 April 2008
Available online 16 April 2008

Keywords:
Kinetics
Isothermal
Thermal decomposition
Cobalt oxalate

ABSTRACT

Thermal decomposition of cobalt oxalate ($CoC_2O_4{\cdot}2H_2O$) was studied using TG, DTA and XRD techniques. Non-isothermal studies revealed that the decomposition occurred in two main stages: removal of water and next decomposition of CoC_2O_4 to Co. Isothermal kinetic studies were conducted for the second stage of decomposition at six different temperatures between 295 and 370 °C in reducing (He + 15 vol% H_2) atmosphere. Kinetic equation was found to obey $g(\alpha) = [-\ln(1-\alpha)]^{1/n} = kt$ relationship with varying values of n between 2 and 4. The variation of activation energy between 73.23 and 119 kJ mol^{-1} from the lowest to the highest temperature of decomposition indicated the multi-step nature of the process. SEM analysis revealed the formation of nano-size powder in this temperature range. Thermal decomposition at 550 °C for 30 min was found to be optimum condition producing fine size, non-pyrophoric and spherical powder in larger scale of production. Both hcp and fcc phases were present in the cobalt powder at room temperature.

1. Introduction

Cobalt is well established for its applications in the field of cemented carbides, tool steels, magnetic materials, paint pigments, catalysts and production of artificial γ-ray sources. Pure cobalt in the form of slugs (6 mm × 25 mm) and pellets (1 mm × 1 mm) are used in the nuclear reactors to prepare Co^{60} γ-radiation source. The key uses of Co^{60} slugs and pellets are food preservation and radiation therapy in medical applications, respectively. These shapes are fabricated through the powder processing route involving appropriate combination of compaction, sintering [1] and hot working techniques, such as hot extrusion, hot swaging under reducing atmosphere. The properties of sintered metallic products depend on the size, morphology and purity of the powders. Various routes such as: (1) aqueous cobaltous hydroxide slurry under hydrogen reduction conditions using palladium chloride catalyst [2], (2) reduction of cobalt oxide, chloride or sulfate [3], (3) decomposition of ammonium cobalt fluoride [4] and (4) electro-winning [3] have been explored for the preparation of cobalt powder.

Thermal decomposition of cobalt oxalate is the most commonly used technique for the preparation of high purity, fine size cobalt metal powder. The co-existence of both hexagonal closed packed (hcp) and face centered cubic (fcc) phases in as produced cobalt powder at room temperature has also been reported earlier [5]. The non-isothermal studies on the mechanism and kinetics of thermal decomposition of cobalt oxalate have been reported earlier [6,7]. However, isothermal kinetics of the decomposition in reducing atmosphere and its effect on powder morphology is not available in the literature. Some isoconversional methods for analyzing thermal decomposition have been described earlier [8,9].

In the present investigation, isothermal kinetics of the decomposition of cobalt oxalate to metallic cobalt powder was studied in a thermogravimetric (TG) and differential thermal analysis (DTA) equipment Setsys Evolution 24, Setaram Instrumentation, France. Based on the non-isothermal studies carried out in both helium and helium +15 vol% H_2 atmospheres, six different temperatures between 295 and 370 °C were selected. The isothermal studies were conducted in the atmosphere containing 15 vol% hydrogen and balance helium. Powder morphology and phase analysis were carried out by SEM and XRD technique, respectively. Co-relation with the larger scale decomposition experiments was established and optimum condition for preparing cobalt powder suitable for making slugs and pellets was predicted.

2. Experimental procedure

2.1. Preparation of cobalt oxalate

99.9% pure cobalt sulfate ($CoSO_4{\cdot}7H_2O$) supplied by M/s s. d. fine chemicals was used as starting feed. Cobalt sulfate solutions

* Corresponding author. Tel.: +91 22 25590183; fax: +91 22 25505151.
E-mail address: sanjib@barc.gov.in (S. Majumdar).

0040-6031/$ – see front matter © 2008 Elsevier B.V. All rights reserved.
doi:10.1016/j.tca.2008.04.005

were prepared by maintaining the cobalt concentration at 30 and 60 g/L. Cobalt oxalate precipitation reactions were conducted by mixing oxalic acid solution with cobalt sulfate solution under vigorous stirring. Studies were conducted by varying the experimental parameters such as temperature, pH and concentration of oxalic acid. The optimum condition producing a maximum cobalt recovery of 99% was found to be *T* 40 °C, pH 1.1 and 40% excess oxalic acid solution. Cobalt oxalate precipitate was filtered, neutralized and dried under infrared lamp. Finally, cobalt oxalate dihydrate ($CoC_2O_4{\cdot}2H_2O$) powder having a pink color was obtained after drying.

2.2. TG–DTA study

Thermogravimetric studies were conducted using the TG–DTA equipment; model SETSYS EVOLUTION 24 from Setaram Instrumentation, France. The equipment consists of cylindrical graphite furnace, graphite reaction tube, TG–DTA sensor (microbalance and DTA transducers), carrier and auxiliary gas inlet, furnace thermocouple for temperature control by PID controller, etc. Tungsten DTA transducer (rod) was used for carrying out the experiments in reducing (He + 15% H_2) as well as inert (pure helium) atmospheres. Criado and Perez-Maqueda [10] have reported that the use of sample controlled thermal analysis (SCTA) methods present two important advantages with regard to the more conventional rising temperature experiments. Because they have a higher resolution power for discriminating among the reaction kinetic models and also is a powered tool for minimizing the influence of the experimental conditions on the forward reaction. In the current study, around 30 mg cobalt oxalate was charged in each experiment in a tungsten (sample) crucible and placed in the housings made in the TG–DTA rod along with the blank reference crucible. The depth of the cobalt oxalate layer inside the crucible was 6 mm. The chamber was evacuated up to 10^{-2} mbar after charging the sample followed by filling with required carrier gas. Initial experiments were conducted under the non-isothermal heating rate of 5 °C min^{-1} up to 550 °C in pure helium (He) and helium +15 vol% hydrogen atmospheres, respectively. Cobalt oxalate produced from both 30 and 60 g/L solutions were studied. The temperature range for the final stage of the decomposition i.e. CoC_2O_4 to Co formation was detected by these initial studies. Next set of experiments was conducted for studying the kinetics of the final stage of decomposition of cobalt oxalate prepared from 60 g/L initial solution under He + 15% H_2 atmosphere. Isothermal decomposition studies were conducted at six different temperatures between 295 and 370 °C. Initially the samples were heated at the rate of 20° min^{-1} to reach the desired temperature of decomposition followed by holding for 4 h at all the different attempted temperatures. The kinetic data obtained from thermogravimetric study was analyzed and activation energy was calculated by establishing the kinetic law.

2.3. Scanning electron microscopy

The particle size and morphology of the cobalt powder was studied in a Hitachi make SEM. Powder was dispersed on a self-adhesive carbon tape and placed inside the chamber of the SEM. The chamber was evacuated to 10^{-5} mbar vacuum and samples were analyzed at 15 kV accelerating voltage and 12.5 mm working distance (WD).

2.4. X-ray diffraction

Panalytical make XRD equipment was used for X-ray diffraction study. Mo Kα radiation of wavelength 0.7093 Å was used and sample scanning was done between the angles of 10–50°. Diffraction peaks were analyzed and indexed according to the diffracting planes of different phases.

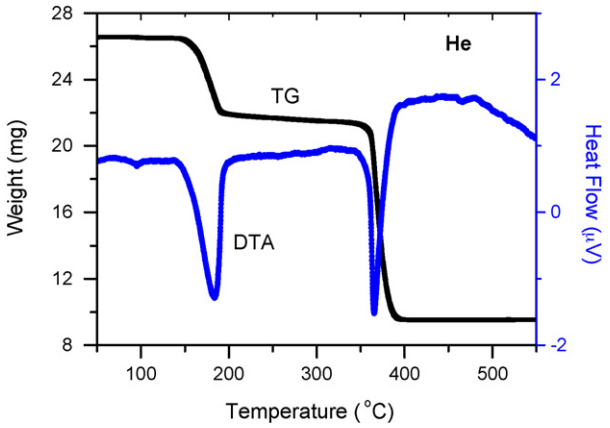

Fig. 1. Decomposition of $CoC_2O_4{\cdot}2H_2O$ in helium. Heating rate 5 °C min^{-1}.

3. Results and discussions

3.1. Non-isothermal studies

TG and DTA data obtained during the decomposition of cobalt oxalate in helium and helium with 15 vol% H_2 are presented in Figs. 1 and 2, respectively. Thermal decomposition of $CoC_2O_4{\cdot}2H_2O$ is described by the following reaction:

$$CoC_2O_4{\cdot}2H_2O = Co + 2CO_2 + 2H_2O \quad (1)$$

As observed in Fig. 1, the decomposition in helium takes place mainly in two stages. In the first stage that takes place below 200 °C water of crystallization gets removed as indicated by a drop in weight and endothermic DTA peak at 182 °C. The second stage is the decomposition of CoC_2O_4 to metallic cobalt and formation of CO_2 gas. The endothermic DTA peak is at 365 °C and the decomposition is complete at 395 °C.

A different nature of the DTA curve (Fig. 2) is observed for decomposition in the atmosphere containing 15 vol% H_2 and balance He. The first stage, removal of water of crystallization showed the similar behavior as obtained in case of He atmosphere, whereas in the second stage there are two additional exothermic peaks at 350 and 372 °C, respectively, coupled with one endothermic peak at 365 °C. The area of the endothermic peak (365 °C) has been reduced because of some other exothermic reactions occurring

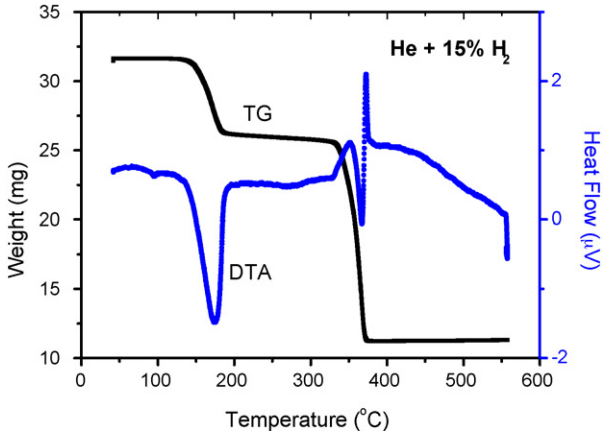

Fig. 2. Decomposition of $CoC_2O_4{\cdot}2H_2O$ in He + 15 vol% H_2. Heating rate 5 °C min^{-1}.

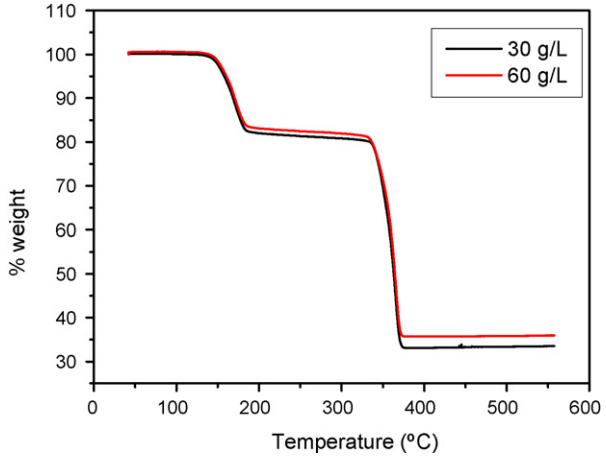

Fig. 3. TG plot for decomposition of oxalate prepared from 30 to 60 g/L sulfate solutions. Heating rate 5 °C min^{-1}.

simultaneously. The gas phase reactions between CO_2 and H_2 forming hydrocarbons are responsible these exothermic peaks. Formation of methane as per the reaction

$$CO_2 + 4H_2 = CH_4 + 2H_2O \quad (2)$$

is thermodynamically feasible ($\Delta G^\circ_r = -13.66$ kcal mol^{-1}) [11] and has been confirmed by Maciejewski et al. [7].

Fig. 3 is the TG plot showing the comparative weight change for the thermal decomposition reactions of cobalt oxalates from 30 to 60 g/L sulfate solutions, respectively. No significant difference in decomposition kinetics is detected though oxalate from 60 g/L solution is expected to have larger particle size. This result has got the significance particularly on the aspects of cobalt metal recovery from the starting feed. It is because the decomposition kinetics is independent of the concentration of the feed solution; the recovery of the cobalt values can be maximized using the feed solution containing highest possible concentration of cobalt. Cobalt oxalate from 60 g/L starting solution was, therefore, used for subsequent studies on isothermal kinetics of second stage of decomposition.

3.2. Isothermal kinetics

Isothermal decomposition studies were conducted in He + 15 vol% H_2 atmospheres to avoid traces of oxygen pick up by the freshly produced cobalt powder. Based on the non-isothermal studies, six different temperatures 295, 310, 325, 340, 355 and 370 °C were selected for conducting isothermal kinetic studies. The samples were heated at 20 °C min^{-1} to the desired temperature followed by isothermal holding for 4 h. Fig. 4 shows the variation of degree of decomposition (α) of CoC_2O_4 to Co with time at different isothermal conditions. Up to the decomposition temperature of 325 °C incubation period is observed and decomposition at 295 °C is not complete within 4 h of holing time. Beyond 340 °C, the decomposition is just initiated and at 370 °C the value of α is 0.05 at $t = 0$. Sigmoidal shape of α–t plot indicates that the kinetics of the decomposition reaches a maximum followed by a decrease in the rate. Reduced time plot approach [12] was used for evaluating the kinetic equation for the decomposition. The kinetic relationship is expressed in the form:

$$g(\alpha) = kt \quad (3)$$

where α is the fraction reacted, k the rate constant and t the time. If $t_{0.5}$ be the time required to obtain 0.5 fraction reacted ($\alpha = 0.5$) then one obtains Eq. (3) in an altered form in terms of dimensionless time

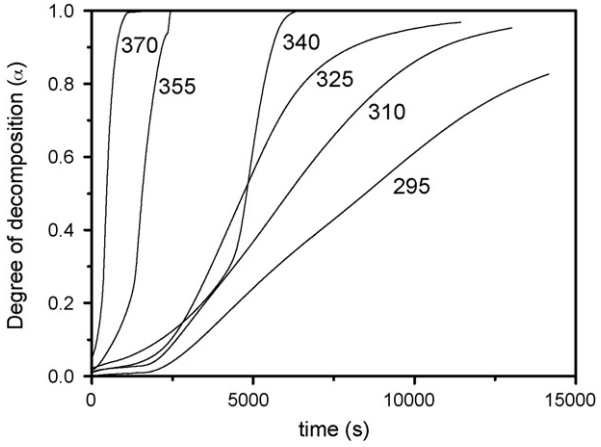

Fig. 4. Kinetic plots for isothermal decomposition.

Table 1
Kinetic models used for plotting $t/t_{0.5}$ vs. α in Fig. 5

Model	Integral form, $g(\alpha)$
A2—Avrami–Erofe'ev (J–M)	$[-\ln(1-\alpha)]^{1/2}$
A3—Avrami–Erofe'ev	$[-\ln(1-\alpha)]^{1/3}$
A4—Avrami–Erofe'ev	$[-\ln(1-\alpha)]^{1/4}$
R2—Contracting area	$1-(1-\alpha)^{1/2}$
R3—Contracting volume	$1-(1-\alpha)^{1/3}$
D1—1D diffusion	α^2
D2—2D diffusion	$(1-\alpha)\ln(1-\alpha)+\alpha$

scale (reduced time)

$$g(\alpha) = A\left(\frac{t}{t_{0.5}}\right) \quad (4)$$

where A is a calculated constant dependent on the form of the function $g(\alpha)$. This expression is independent of the kinetic rate constants and is dimensionless. Calculations were performed for evaluating $t/t_{0.5}$ at different values of α for different temperatures. The values were compared with standard values for different kinetic models [13].

The reduced time plots for the decomposition kinetics at 295 and 310 °C are presented in Fig. 5 along with the theoretical plots for different classical models (Table 1). At lower decomposition temperatures (295 and 310 °C), the experimental curves are closely matching with the equation $[-\ln(1-\alpha)]^{1/2} = kt$ (A2). The model for

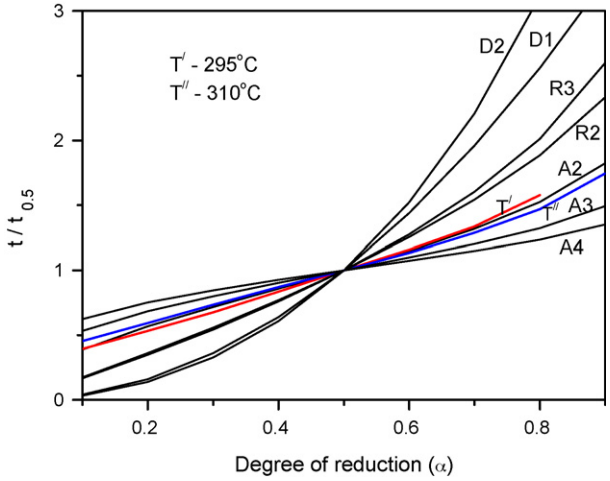

Fig. 5. Reduced time plots for different kinetic models and experimental conditions.

Table 2
Residual sum of squares (s^2) for the kinetic data obtained at different isothermal experimental conditions for different kinetic models

Temp (°C)	A2	A3	A4	R2	R3
295	0.00113[a]	0.339388	0.303281	0.813425	1.018416
310	0.002237[a]	0.016221	0.043416	0.111119	0.190598
325	0.018291	0.003946[a]	0.017089	0.175287	0.26832
340	0.105476	0.027427	0.013298[a]	0.368703	0.509876
355	0.050805	0.005104	0.005037[a]	0.26031	0.37762
370	0.01015[a]	0.011171	0.032828	0.142792	0.231028

[a] Minimum s^2 values.

this equation known as J–M model named after Johnson and Mehl [14], is well known and commonly used to describe the kinetics of recrystallization [15].

For obtaining the kinetic equation at higher temperatures, a statistical test has been performed for different kinetic models and residual sum of squares (s^2) given by

$$s^2 = \frac{1}{n-1}\sum\left(\frac{t}{t_{0.5}} - \frac{g(\alpha)}{g(\alpha_{0.5})}\right)^2 \quad (5)$$

for each model has been calculated for different temperatures and presented in Table 2. It is observed that at lower temperatures (295 and 310 °C), s^2 is minimum for A2 whereas the minimum residual sum of squares at 325, 340, 355 and 370 °C was observed for the models A3, A4, A4 and A2, respectively, as indicated by asterisk (*) marks in Table 2.

Therefore, thermal decomposition of cobalt oxalate follows Avrami–Erofe'ev model

$$g(\alpha) = [-\ln(1-\alpha)]^{1/n} = kt \quad (6)$$

where the exponent '*n*' varies between 2 and 4 with increase in the decomposition temperature.

The value of activation energy was calculated by plotting $\ln t_\alpha$ against $1/T$ as because the decomposition was not following any particular kinetic law throughout the temperature range. Fig. 6 represents a typical $\ln t_\alpha$ vs. $1/T$ plot for $\alpha = 0.4$. From the slope of linear curve, the activation energy at $\alpha = 0.4$ was found to be 93.8 ± 8.31 kJ mol^{-1}. Similarly, the values of activation energy at different α were calculated by analyzing $\ln t_\alpha$ vs. $1/T$ plots for different α. Fig. 7 shows the variation of activation energy (E_α) with the extent of conversion (α). The increase in E_α with α indicates that the thermal decomposition of cobalt oxalate to cobalt is a multi-step process [16,17]. The activation energy varied between 73.23 and 119 kJ mol^{-1} from the lowest to the highest temperature of decomposition conditions.

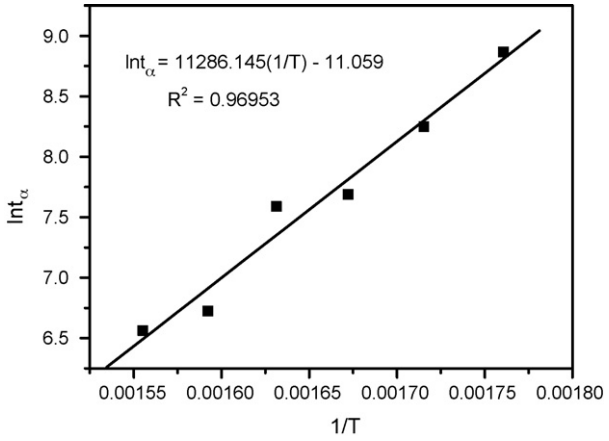

Fig. 6. Plot of $\ln t_\alpha$ vs. $1/T$ for $\alpha = 0.4$.

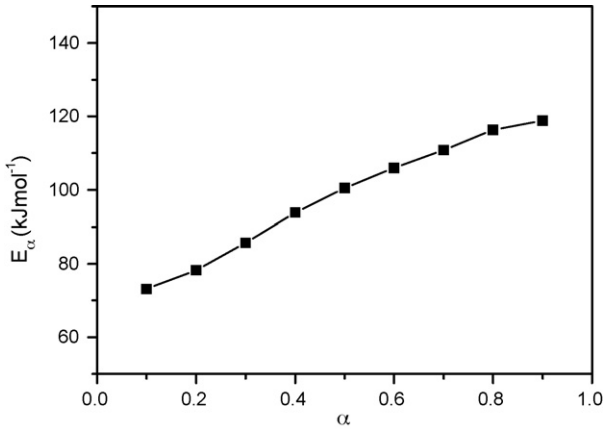

Fig. 7. Dependence of activation energy on the extent of conversion (α). E_α values obtained from $\ln t_\alpha$ vs. $1/T$ plots.

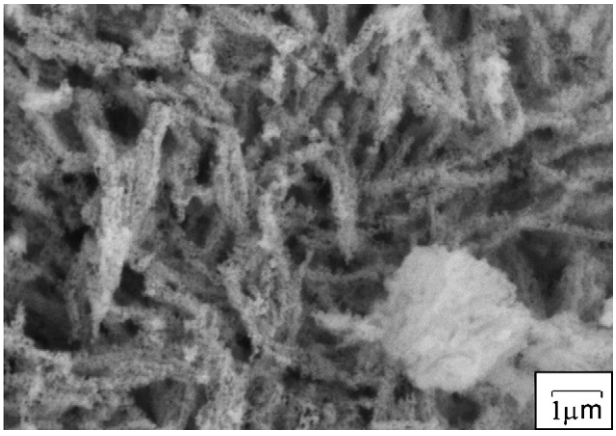

Fig. 8. SEM image showing nano-size cobalt powder formation at 340 °C.

3.3. Morphology and phase of cobalt

Detailed SEM analysis of the cobalt powder produced at different isothermal conditions was carried out. The powder produced below 340 °C immediately caught fire while removing from the thermobalance. Since during the decomposition of the cobalt oxalate particle six foreign atoms leave its lattice for each cobalt atom, the product becomes porous thus having a very high specific surface

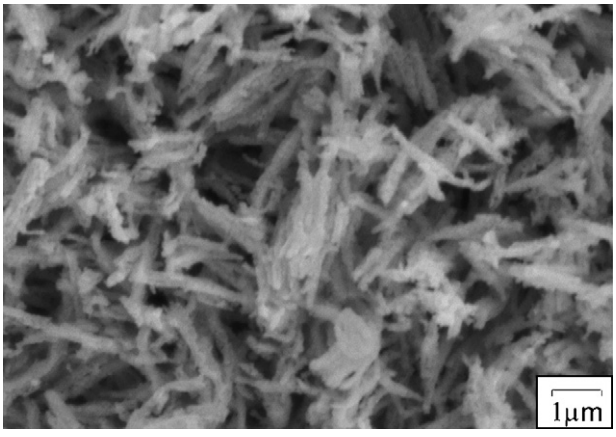

Fig. 9. SEM image showing nano-powder chain formation at 370 °C.

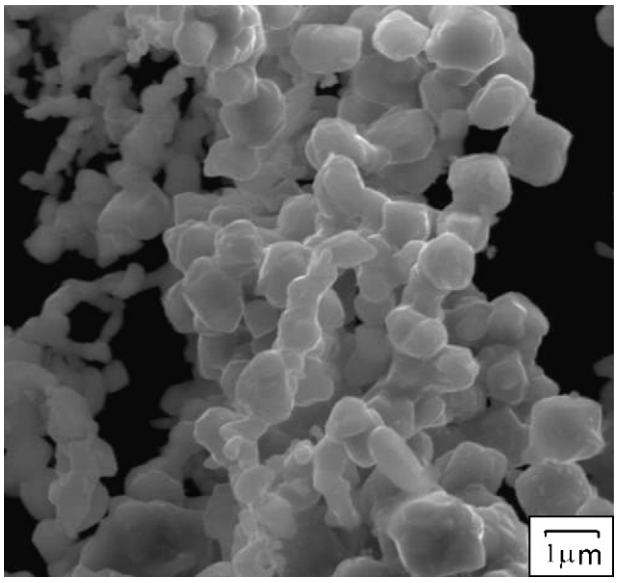

Fig. 10. Micron size cobalt powder produced after decomposition at 550 °C for 30 min.

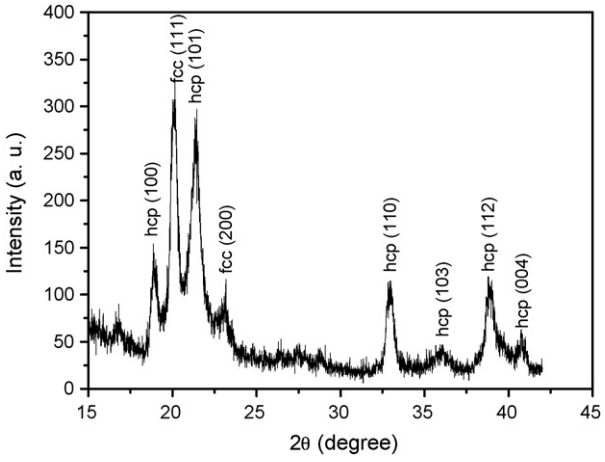

Fig. 11. XRD plot showing co-existence of both hcp and fcc phases in cobalt powder.

area. This makes the powder highly pyrophoric in nature. Fig. 8 shows the SEM image of the cobalt powder produced at 340 °C. The individual particle size was less than 100 nm which is the single domain region of metallic cobalt. It becomes very difficult to separate or resolve individual cobalt particles of this nano-size range.

As the temperature of decomposition is increased to 370 °C, coarsening of the fine particles takes place. As evident in Fig. 9, cobalt crystallite size is bigger than that produced at 340 °C. The highly ferromagnetic character of the powder makes them aligned at particular directions. As a result the acicular morphology of the aggregate is observed in all the powders. From the point of view of larger scale production, the powder is still difficult to handle.

Larger scale (60 g) experiments were conducted in a horizontal tubular furnace keeping the cobalt oxalate powder in a molybdenum tray. Temperature and time of decomposition was varied starting from 400 °C. The optimum condition producing non-pyrophoric, spherical powder of minimum agglomeration was found to be as temperature 550 °C, time 30 min under reducing atmosphere. Fig. 10 shows the formation of 1–1.5 μm spherical powder at the optimized conditions. The powder was easily flowable and thus suitable for preparation of cobalt slugs and pellets by powder metallurgical processes. Fig. 11 is the XRD plot of the cobalt powder produced at 550 °C showing the presence of both hcp and fcc phases in the powder. Strong (1 1 1) reflections from fcc cobalt was detected along with the (1 0 0), (1 0 1), etc., hcp reflections. Though the allotropic transition from hcp to fcc phase is at 417 °C, significant amount of high temperature fcc phase is retained in the cobalt crystals. The peak broadening at each reflection is also the indicative of formation of fine size cobalt powder.

4. Conclusions

Isothermal kinetics of thermal decomposition of cobalt oxalate to cobalt was found to obey Avrami-Erofe'ev equations. The increase in activation energy with increasing temperature revealed that the decomposition involved multi-step reaction mechanisms. The powder size was less than 100 nm at the decomposition temperatures below 370 °C. Decomposition at 550 °C for 30 min produced the cobalt powder suitable for making slugs and pellets by powder metallurgical processing techniques. Existence of both hcp and fcc phases was observed in the cobalt powder at room temperature.

Acknowledgements

The authors wish to thank Prof. I. Samajdar and Dr. S. L. Kamat of Indian Institute of Technology Bombay, Powai, Mumbai, India for extending his help in carrying out XRD and SEM experiments, respectively.

References

[1] S. Majumdar, I.G. Sharma, R. Kapoor, J.K. Chakraborty, A.K. Suri, Metall. Mater. Trans. B 37 (2006) 633–639.
[2] D.J. Kim, H.S. Chung, K. Yu, Mater. Res. Bull. 37 (2002) 2067–2075.
[3] K.K. Sharma, T.V.L. Narshima Rao, Non-Ferrous Metals Strategy Cum Source Book, 4, 2003, pp. 175–187.
[4] I.G. Sharma, P. Alex, S. Majumdar, J. Kishor, A.K. Suri, J. Alloy. Compd. 437 (2007) 231–237.
[5] J.Y. Huang, Y.K. Wu, H.Q. Ye, Appl. Phys. Lett. 66 (1995) 308–310.
[6] B. Malecka, E. Drozdz-Ciesla, A. Malecki, J. Therm. Anal. Cal. 60 (2002) 819–831.
[7] M. Maciejewski, E. Ingier-Stocka, W.D. Emmerich, A. Baiker, J. Therm. Anal. Cal. 60 (2000) 735–758.
[8] S. Vyazovkin, W. Linert, J. Solid State Chem. 114 (1995) 392–398.
[9] P.J. Skrdla, R.T. Robertson, Thermochim. Acta 453 (2007) 14–20.
[10] J.M. Criado, L.A. Perez-Maqueda, J. Therm. Anal. Cal. 80 (2005) 27–33.
[11] I. Barin, O. Knacke, Thermochemical Properties of Inorganic Substances, Springer-Verlag Berlin Heidelberg, New York, 1973.
[12] H.S. Ray, Kinetics of Metallurgical Reactions, Oxford & IBH Publishing Co. Pvt. Ltd., 1990, pp. 39–45.
[13] E.M. Kurian, J. Therm. Anal. 35 (1989) 1111–1117.
[14] W.A. Johnson, R.F. Mehl., Trans. AIME 135 (1939) 416–441.
[15] F.J. Humphreys, M. Hatherly, Recrystallization and Related Annealing Phenomena, Pergamon Press, Oxford, 1995, pp. 188–189.
[16] S. Vyazovkin, N. Sbirrazzuoli, J. Phys. Chem. B 107 (2003) 882–888.
[17] M.E. Brown, M. Maciejewski, S. Vyazovkin, R. Nomen, J. Sempere, A. Burnham, J. Opfermenn, R. Strey, H.L. Anderson, A. Kemmler, R. Keuleers, J. Janssens, H.O. Desseyn, C.-R. Li, T.B. Tang, B. Roduit, J. Malek, T. Mitsuhashi, Thermochim. Acta 355 (2000) 125–143.